Int. J. Heat Mass Transfer. Vol. 25, No. 2, pp. 290–293, 1982
Printed in Great Britain

0017-9310/82/020290-04 $03.00/0
Pergamon Press Ltd.

HEAT AND MASS TRANSFER IN UNSTEADY COMPRESSIBLE AXISYMMETRIC STAGNATION POINT BOUNDARY LAYER FLOW OVER A ROTATING BODY

M. KUMARI and G. NATH
Department of Applied Mathematics, Indian Institute of Science, Bangalore 560012, India

(*Received* 28 *May* 1979 *and in revised form* 25 *September* 1980)

NOMENCLATURE

a,	constant having a dimension $(\text{time})^{-1}$;
A,	dimensionless constant;
C_f, $\bar{C}_f$,	skin friction coefficients in the x and y directions, respectively;
f,	dimensionless stream function;
f_w,	surface mass transfer parameter;
F, s,	dimensionless velocity components in the x and y directions, respectively;
F'_w, s'_w,	surface velocity gradients in the x and y directions, respectively;
$\bar{F}'_w$, S'_w,	surface skin friction parameters in the x and y directions, respectively;
g,	dimensionless enthalpy;
g_w,	enthalpy at the wall at time $t^* = 0$;
g'_w, G'_w,	enthalpy gradient and heat transfer parameter at the surface, respectively;
h,	enthalpy;
h_{w0},	value of h_w at $t^* = 0$;
N,	ratio of the density–viscosity product;
Pr,	Prandtl number;
q_w,	heat transfer rate at the wall;
r,	distance from the axis of the body of revolution ($r \simeq x$ near the stagnation point);
Re_x,	local Reynolds number;
St,	Stanton number;
t, t^*,	dimensional and dimensionless times, respectively;
u, v, w,	velocity components in the x, y and z directions, respectively;
x, y, z,	longitudinal, tangential and normal directions, respectively.

Greek symbols

$\varepsilon, \varepsilon_1, \varepsilon_2, \varepsilon_3$,	constants (positive);
η,	dimensionless similarity variable;
λ,	dimensionless rotation parameter;
μ,	viscosity;
ν,	kinematic viscosity;
ρ,	density;
τ_x, τ_y,	shear stresses in the x and y directions, respectively;
ϕ, ϕ_1, ϕ_2,	functions of t^*;
ω,	index of the power-law variation of viscosity;
ω_1,	angular velocity at $t^* = 0$;
ω^*,	frequency parameter.

Superscript

$'$,	denotes differentiation with respect to η.

Subscripts

e,	denotes conditions at the edge of the boundary layer;
w,	denotes conditions at the surface $z = \eta = 0$;
0,	denotes conditions at the stagnation point.

1. INTRODUCTION

THE FLOW, heat and mass transfer characteristics of the unsteady laminar compressible stagnation-point boundary layer over a rotating body of revolution are important in re-entry problems of spacecrafts and missiles. To the authors' knowledge, no detailed analysis of this problem is presented in the literature. However, particular cases of the above problem in which either the flow is steady or the body is stationary have been studied by a number of investigators [1–3].

The aim of the present analysis is to study the unsteady laminar compressible stagnation-point boundary layer flow over a rotating body of revolution (sphere) with mass transfer when the free-stream velocity, the rotation of the body, the surface mass transfer, and the wall temperature vary arbitrarily with time. The effect of the variation of the density–viscosity product across the boundary layer has been included in the analysis. The partial differential equations governing the flow have been solved numerically using an implicit finite difference scheme [4, 5]. The results have been compared with the existing results wherever available [3, 6]. This analysis is relevant to the heat transfer problem for large re-entry vehicles, because it was shown by Scala and Workman [1] that the effect of moderate rotation on the heat transfer is not significant for small re-entry vehicles.

2. GOVERNING EQUATIONS

We consider the unsteady laminar compressible boundary layer flow at the stagnation point of a rotating body of revolution (sphere) with variable gas properties ($\rho \propto T^{-1}$, $\mu \propto T^{\omega}$, $Pr = 0.72$) and with mass transfer under the assumptions that the incident stream, rotation of the body, surface mass transfer and wall temperature vary arbitrarily with time. It is also assumed that the dissipation terms are negligible at the stagnation point and the external flow is homentropic. The equations governing the above flow can be expressed in dimensionless form as [1, 3, 5]

$$(NF')' + \phi f F' + 2^{-1}[\phi(g - F^2) + \phi^{-1}(\mathrm{d}\phi/\mathrm{d}t^*)(g - F) + \lambda^2\phi^{-1}\phi_1^2 s^2 - \partial F/\partial t^*] = 0, \quad (1a)$$

$$(Ns')' + \phi f s' - 2^{-1}[2\phi F s + \phi_1^{-1}(\mathrm{d}\phi_1/\mathrm{d}t^*)s + \partial s/\partial t^*] = 0, \quad (1b)$$

$$Pr^{-1}(Ng')' + \phi f g' - 2^{-1}\partial g/\partial t^* = 0. \quad (1c)$$

The boundary conditions are:

$$\left.\begin{aligned} &F=0,\ s=1,\ g=g_w\phi_2(t^*)\ \text{for}\ \eta=0 \\ &F=g=1,\ s=0\ \ \text{as}\ \eta\to\infty \end{aligned}\right\}\ \text{at}\ t^*\geqslant 0. \tag{2}$$

It is assumed here that initially the flow is steady and then changes to unsteady at $t^* > 0$. Hence, the initial conditions for F, s and g at $t^* = 0$ are given by the steady-flow equations obtained by putting

$$\begin{aligned} &\phi(t^*) = \phi_1(t^*) = \phi_2(t^*) = 1, \\ &\mathrm{d}\phi/\mathrm{d}t^* = \mathrm{d}\phi_1/\mathrm{d}t^* = 0,\ \partial/\partial t^* = 0 \end{aligned} \tag{3}$$

in equation (1). Here the condition $\partial/\partial t^* = 0$ at $t^* = 0$ implies that all the derivatives of the dependent variables with respect to t^* vanish. Consequently, the initial conditions (i.e. steady state equations) can be expressed as

$$(NF')' + fF' + 2^{-1}(g - F^2 + \lambda^2 s^2) = 0, \tag{4a}$$

$$(Ns')' + fs' - Fs = 0, \tag{4b}$$

$$Pr^{-1}(Ng')' + fg' = 0. \tag{4c}$$

Here

$$\eta = 2^{1/2}(\rho_e a/\mu_e)^{1/2}\int_0^z (\rho/\rho_e)\,\mathrm{d}z,\ t^* = at, \tag{5a}$$

$$u = ax\phi(t^*)F(\eta, t^*),\ v = \omega_1 x\phi_1(t^*)s(\eta, t^*),$$

$$w = -2^{-1/2}(\rho_e/\rho)(\mu_e a/\rho_e)^{1/2}[2\phi(t^*)f(\eta, t^*) + \partial\eta/\partial t^*],$$

$$h/h_e = g(\eta, t^*),\ F(\eta, t^*) = f'(\eta, t^*), a = (\mathrm{d}u_e/\mathrm{d}x)_{t^*=0}, \tag{5b}$$

$$u_e = ax\phi(t^*),\ N = \rho\mu/\rho_e\mu_e = g^{\omega-1},\ \lambda = \omega_1/a,$$

$$f = \int_0^\eta F\,\mathrm{d}\eta + f_w, f_w = A/\phi(t^*), \tag{5c}$$

$$A = -2^{-1/2}(Re_x)^{1/2}[(\rho w)_w/\rho_e(u_e)_{t^*=0}],\ Re_x = ax^2/\nu_e. \tag{5d}$$

It may be noted that for a stationary body, $\lambda = 0$ and equation (1b) becomes inessential since s is not interesting in this case. We note that for the axisymmetric stagnation point flow, without loss of generality, the free-stream velocity distribution u_e can be taken to be of the form given by equation (5c). It may be remarked that $\omega = 0.5$ for high-temperature flows, $\omega = 0.7$ for low-temperature flows, and $\omega = 1$ represents the simplification of a constant density–viscosity product [7]. Both ϕ and ϕ_1 are arbitrary functions of time representing the nature of the unsteadiness in the external stream and in the rotation of the body, respectively, and have a continuous first derivative for $t^* \geqslant 0$. Here the normal velocity at the wall $(\rho w)_w$ is selected in such a way that $(\rho w)_w/[\rho_e(u_e)_{t^*=0}]$ is a constant and hence A can be considered as a constant ($A \gtrless 0$ according to whether there is suction or injection). Consequently, the mass transfer parameter f_w varies as $\phi^{-1}(t^*)$.

The skin friction coefficients in the x and y directions and heat transfer coefficient are given by

$$C_f = 2\tau_x/[\rho_e(u_e^2)_{t^*=0}] = 2^{3/2} \times (Re_x)^{-1/2}\phi(t^*)\phi_2^{\omega-1}(t^*)\bar{F}'_w, \tag{6a}$$

$$\bar{C}_f = 2\tau_y/[\rho_e(u_e^2)_{t^*=0}] = 2^{3/2} \times (Re_x)^{-1/2}\lambda\phi(t^*)\phi_2^{\omega-1}(t^*)S'_w, \tag{6b}$$

$$St = q_w/[(h_e - h_{w0})\rho_e(u_e)_{t^*=0}] = 2^{1/2}(Re_x)^{-1/2}Pr^{-1}(1 - g_w)^{-1}\phi_2^{\omega-1}(t^*)G'_w. \tag{6c}$$

where

$$\tau_x = \mu_w(\partial u/\partial z)_w,\ \tau_y = \mu_w(\partial v/\partial z)_w, \tag{7a}$$

$$q_w = \mu_w Pr^{-1}(\partial h/\partial z)_w,\ \bar{F}'_w = g_w^{\omega-1}F'_w,$$

$$S'_w = g_w^{\omega-1}s'_w,\ G'_w = g_w^{\omega-1}g'_w. \tag{7b}$$

3. RESULTS AND DISCUSSION

The set of equations (1) was solved numerically under boundary conditions (2) and initial conditions (4) using an implicit finite difference scheme which has been fully described by Marvin and Sheaffer [4] and Vimala and Nath [5]. Hence, for the sake of brevity, it is not presented here. We have considered the following distributions of the free-stream velocity rotation of the body and wall temperature:

$$\begin{aligned} &\phi(t^*) = 1 + \varepsilon(t^*)^2,\ \phi(t^*) = 1 + \varepsilon_1\sin^2(\omega^* t^*), \\ &\phi_1(t^*) = 1 + \varepsilon_2(t^*)^2,\ \phi_2(t^*) = 1 - \varepsilon_3 t^*. \end{aligned} \tag{8}$$

Computations were carried out for various values of the parameters characterizing the problem. To ensure the convergence of the finite difference scheme to the true solution, several values of the step size $\Delta\eta$ and Δt^* were employed and optimum values of $\Delta\eta(\Delta\eta = 0.02)$ and Δt^* ($\Delta t^* = 0.05$) were obtained.

In order to test the accuracy of the present method, the skin friction and heat transfer results for the steady flow over a stationary body ($\lambda = 0$) in the absence of mass transfer ($A = 0$) have been compared with those of Bade [6] and for the unsteady flow with those of Meena [3] and they are found to be in excellent agreement (the comparison is not shown here for the sake of brevity). We have also compared our skin friction and heat transfer results for the unsteady flow over a 2-dim. body (cylinder) with those of series solution method [8] and we find that the series solution method overestimates the fluctuations of the skin friction and heat transfer over the steady mean (see Fig. 1). The difference between the two results is more pronounced for skin friction than for heat transfer.

Some representative skin friction and heat transfer results ($\bar{F}'_w$, $-S'_w$, G'_w) for constantly accelerating free-stream velocity distribution $\phi(t^*) = 1 + \varepsilon(t^*)^2$ have been presented in Figs. 2(a–c). These figures show that the body rotation parameter has strong effect on the skin friction parameters $\bar{F}'_w$ and $-S'_w$ whereas its effect on the heat transfer parameter G'_w is rather weak. The reason for this weak dependence is that the dissipation parameter near the stagnation point has been neglected as it is considered to be small. Furthermore, the variation of the density–viscosity product across the boundary layer ($\omega \neq 1$) for the rotating body ($\lambda \neq 0$) exerts a strong influence on $\bar{F}'_w$, $-S'_w$ and G'_w whereas its effect on them when $\lambda = 0$ (stationary body) is relatively weak. The effects of the time-dependent rotation of the body ($\phi_1(t^*) = 1 + \varepsilon_2(t^*)^2$, $\varepsilon_2 > 0$) and constant rotation of the body ($\phi_1(t^*) = 1$) on $\bar{F}'_w$,

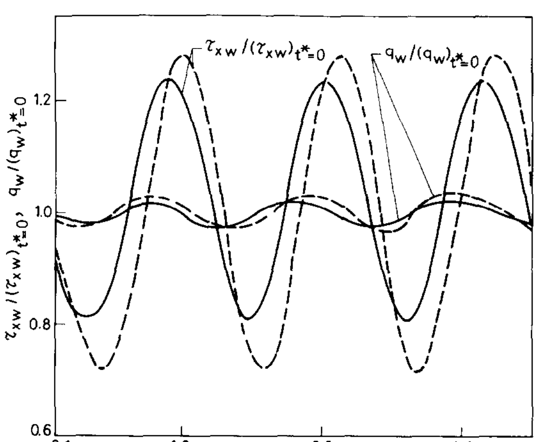

FIG. 1. Comparison of skin friction and heat transfer results for a cylinder with series solution (dashed lines) for $\phi(t^*) = 1 + \varepsilon_1\cos(\omega^* t^*)$, $\lambda = 0$, $g_w = 2.003$, $\omega = 1.0$, $Pr = 0.714$, $\omega^* = 5.6$, $\varepsilon_1 = 0.1$.

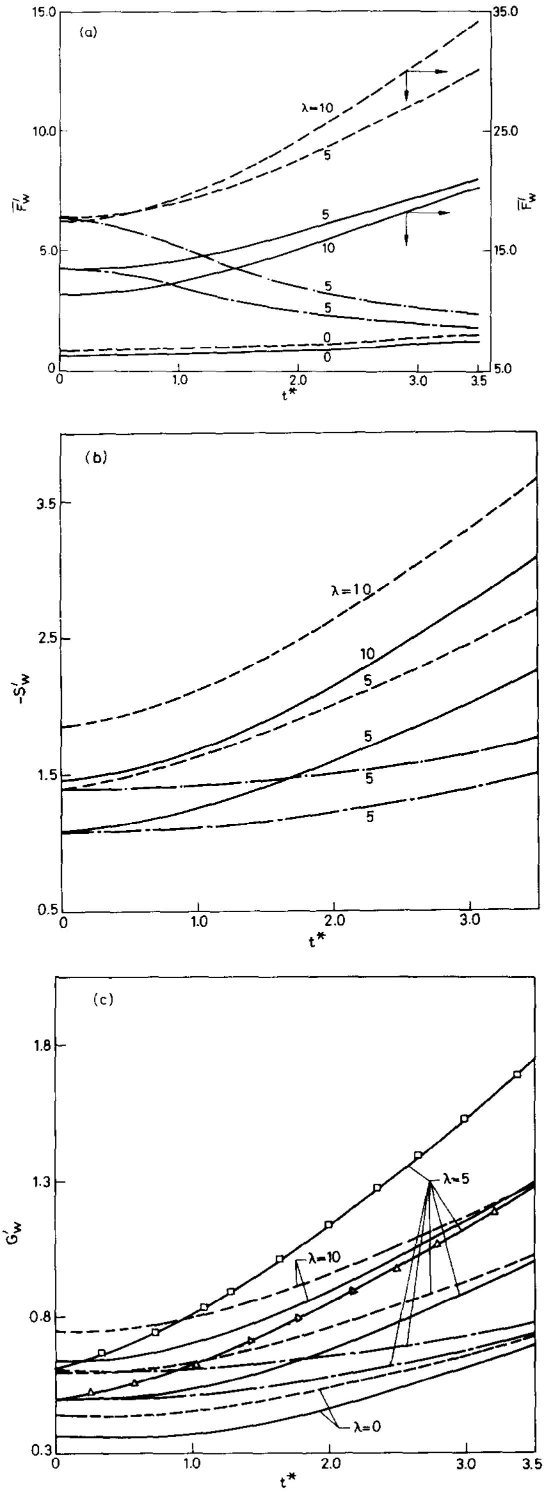

FIG. 2. (a) Skin friction parameter in the x direction $\bar{F}'_w$, (b) skin friction parameter in the y direction $-S'_w$ and (c) heat transfer parameter G'_w for $g_w = 0.2, \lambda = 0, 5$ and $10, A = 0, Pr = 0.72$. $\phi(t^*) = 1 + \varepsilon(t^*)^2\ (t^* \geq 0); \varepsilon = \varepsilon_2 = 0.25; \varepsilon_3 = 0.05$. ——, $\omega = 1.0, \phi_1(t^*) = 1 + \varepsilon_2(t^*)^2\ (t^* \geq 0), \phi_2(t^*) = 1.0$; - - -, $\omega = 0.5, \phi_1(t^*) = 1 + \varepsilon_2(t^*)^2, (t^* \geq 0), \phi_2(t^*) = 1.0$; ——-——, $\omega = 1.0, \phi_1(t^*) = \phi_2(t^*) = 1.0$; ——·——, $\omega = 0.5, \phi_1(t^*) = \phi_2(t^*) = 1.0$; ——△——, $\omega = 1.0, \phi_1(t^*) = 1 + \varepsilon_2(t^*)^2, \phi_2(t^*) = 1 - \varepsilon_3 t^*\ (t^* \geq 0)$; ——□——, $\omega = 0.5, \phi_1(t^*) = 1 + \varepsilon_2 t^{*2}, \phi_2(t^*) = 1 - \varepsilon_3 t^* (t^* \geq 0)$.

$-S'_w$ and G'_w are also shown in Figs. 2(a, b). These figures indicate that the values of $\bar{F}'_w$, $-S'_w$ and G'_w for $\phi_1(t^*) = 1 + \varepsilon_2(t^*)^2$ are greater than those for $\phi_1(t^*) = 1$. We also find that for $\phi_1(t^*) = 1$, $\bar{F}'_w$ decreases as t^* increases, whereas it increases for $\phi_1(t^*) = 1 + \varepsilon_2(t^*)^2$. This difference in behaviour is due to the net increase or decrease in the boundary layer thickness with time. It is well known that the rotation of the body decreases the thickness of the boundary layer, but it (boundary-layer thickness) increases with time. The effect of the variation of the wall temperature with time ($\phi_2(t^*) = 1 - \varepsilon_3 t^*$) is appreciable only on G'_w (Fig. 2c) whereas its effect on $\bar{F}'_w$ and $-S'_w$ is small and they are almost coincident with those of constant wall-temperature case [$\phi_2(t^*) = 1$] on the scale used here, and therefore they are not shown here.

The effect of mass transfer on $\bar{F}'_w$, $-S'_w$ and G'_w for $\phi(t^*) = 1 + \varepsilon(t^*)^2$ has also been studied (not shown in figures for lack of space†). As expected, suction ($A > 0$) increases $\bar{F}'_w$, $-S'_w$ and G'_w whereas injection ($A < 0$) does the opposite. The effect of suction or injection is more pronounced on G'_w and $-S'_w$ than on $\bar{F}'_w$.

It is evident from the results for $\phi(t^*) = 1 + \varepsilon_1 \sin^2(\omega^* t^*)$ that the skin friction parameters $\bar{F}'_w$ and $-S'_w$ respond more to the fluctuations of the free-stream velocity as compared to the heat transfer parameter G'_w.†

It has been observed that there is a velocity overshoot in the longitudinal velocity profiles F for $\lambda > 0$ (rotating body) and the velocity overshoot is reduced as ω increases from 0.5 to 1.0 or t^* increases.† Similar effects have been observed by Back [9] for the steady state case in an analogous situation where the fluid is rotating and the body is stationary. However, no velocity overshoot occurs when $\lambda = 0$ (stationary body) whatever may be the values of the other parameters which is the same as observed by Bade [6]. The reason for the occurrence of the velocity overshoot can be explained as follows. The flow in the boundary layer and in the free stream is subjected to the same longitudinal pressure gradient $(-\partial p/\partial x = \rho_e\, \partial u_e/\partial t^* + \rho_e u_e\, \partial u_e/\partial x)$. However, in the boundary layer, viscous effects reduce the tangential velocity and thus the acceleration term $(\rho v^2/x)$. Consequently, the longitudinal pressure gradient causes larger longitudinal flow acceleration to occur in the boundary layer than that present without tangential velocity even though the shear stress tends to balance the longitudinal pressure gradient near the surface.

4. CONCLUSIONS

The rotation of the body exerts a strong influence on the skin friction, but its effect on the heat transfer is comparatively weak. On the other hand, the effect of the variation of the wall temperature with time [$\phi_2(t^*) = 1 - \varepsilon_3 t^*, t^* \geq 0$] on the heat transfer is appreciable whereas the skin friction is very little affected by it. The variation of the density–viscosity product across the boundary layer strongly affects both the skin friction and heat transfer. Suction increases the skin friction and heat transfer but injection does the reverse. There is a velocity overshoot in the longitudinal velocity profiles which increases as the rotation of the body increases.

REFERENCES

1. S. M. Scala and J. B. Workman, The stagnation-point boundary layer on a rotating hypersonic body, *J. Aerospace Sci.* **26**, 183 (1959).
2. D. P. Telionis and T. R. Gupta, Compressible oscillating boundary layers, *AIAA Jl* **15**, 974–983 (1977).
3. B. K. Meena, Analysis of some laminar boundary layer flows by numerical methods. Ph.D. thesis, Indian Institute of Science, Ch. 2 (1978).

† The results may be obtained from the authors.

4. J. G. Marvin and Y. S. Sheaffer, A method for solving nonsimilar laminar boundary-layer equations including foreign gas injection, NASA TN D-5516 (1969).
5. C. S. Vimala and G. Nath, Unsteady laminar boundary layers in a compressible stagnation flow, *J. Fluid Mech.* **70**, 561–572 (1975).
6. W. L. Bade, Stagnation-point heat transfer in a high-temperature inert gas, *Phys. Fluids* **5**, 150–154 (1962).
7. J. F. Gross and C. F. Dewey, Similar solutions of the laminar boundary layer equations with variable properties, *Fluid Dynamics Transactions* Vol. 2, p. 529. Pergamon Press, Oxford (1965).
8. R. J. Gribben, The fluctuating flow of a gas near a stagnation point on a hot wall, *J. appl. Mech.* **38**, 820–828 (1971).
9. L. H. Back, Flow and heat transfer in laminar boundary layers with swirl, *AIAA Jl* **7**, 1781–1789 (1969).

Int. J. Heat Mass Transfer. Vol. 25, No. 2, pp. 293–297, 1982
Printed in Great Britain
0017-9310/82/020293-05 $03.00/0

NATURAL CONVECTION HEAT TRANSFER COEFFICIENTS MEASURED IN EXPERIMENTS ON FREEZING

E. M. SPARROW and P. SOUZA MENDES
Department of Mechanical Engineering, University of Minnesota, Minneapolis, Minnesota 55455, U.S.A.

(*Received* 1 *April* 1981 *and in revised form* 9 *June* 1981)

NOMENCLATURE

- g, gravitational acceleration;
- h, local heat transfer coefficient at solid–liquid interface;
- k, thermal conductivity of liquid phase;
- k_s, thermal conductivity of solid phase;
- Nu_x, local Nusselt number, hx/k;
- n, normal to interface;
- Pr, Prandtl number;
- Ra_x, local Rayleigh number, $[g\beta(T_0 - T^*)x^3/\nu^2]Pr$;
- r, radial coordinate;
- r_w, radius of cooled tube;
- T, temperature;
- T_0, wall temperature of containment vessel;
- T_w, wall temperature of cooled tube;
- T^*, fusion temperature;
- T_∞, temperature outside of boundary layer;
- x, axial coordinate measured downward along cooled tube.

Greek symbols

- β, coefficient of thermal expansion;
- δ, local thickness of frozen layer;
- ν, kinematic viscosity.

INTRODUCTION

IT IS NOW well established that natural convection plays a key role in both freezing and melting processes [1]. In the case of freezing, natural convection occurs in the unfrozen liquid into which the solidification front advances, provided that the temperature of the liquid exceeds the phase-change temperature. For melting, natural convection will occur in the liquid melt, except, perhaps, for very thin melt layers where heat is transferred by conduction alone.

For either freezing or melting, the liquid-filled volume in which the natural convection takes place is not of elementary shape (such as, for example, rectangular or annular enclosures). The non-elementary nature of these liquid volumes is related to the fact that at least one of the boundaries of the volume is the phase-change interface. In the presence of natural convection, the interface is, generally, a curved surface which does not coincide with a coordinate surface (e.g., a surface where one of the coordinates is constant). Another feature of the phase-change interface is that its shape may change with time as freezing or melting progresses. As a consequence of the shape of the liquid volume, it appears that the heat transfer coefficients needed for the analysis of natural convection-affected phase change cannot be taken directly from the literature on natural convection in single-phase systems where relatively regularly shaped domains have been considered.

Natural convection heat transfer coefficients specific to melting have been investigated experimentally to a moderate extent and, aside from the recent experiments of [2], this work has been brought together in [1]. In addition, numerical solutions for the conjugate conduction–natural convection problem associated with melting about a vertical cylinder have been carried out [3,4]. On the other hand, as is apparent from [1], there is a paucity of work on natural convection heat transfer coefficients related to freezing.

The present paper reports on natural convection heat transfer coefficients measured in experiments on freezing about a cooled vertical tube which is situated in a liquid phase-change medium that is maintained at a temperature above the fusion value.

THE EXPERIMENTS

The apparatus used for the experiments is an adaptation of that employed in an earlier study with different objectives [5]. In order to facilitate the subsequent presentation and discussion of the results, it is useful to give a brief description of the apparatus here.

Figure 1 is a schematic drawing of the apparatus with a data run in progress. The main components of the apparatus are: (1) a cylindrical containment vessel for the phase-change medium, (2) a constant temperature water bath which serves as an isothermal environment for the containment vessel and which maintains the surface temperature of the vessel at a constant value T_0 that is higher than the fusion temperature T^*, and (3) a circular tube which is positioned along the axis of the containment vessel during a data run and which is water-cooled so that its surface temperature T_w is lower than